Monte Carlo Investigations of Solvent Effects on the Chorismate to Prephenate Rearrangement

Heather A. Carlson and William L. Jorgensen*

Contribution from the Department of Chemistry, Yale University, New Haven, Connecticut 06520-8107

Received May 6, 1996. Revised Manuscript Received July 15, 1996[⊗]

Abstract: Monte Carlo simulations have been used to determine changes in free energies of solvation for the rearrangement of chorismate to prephenate in water and methanol. Structures and partial charges from the ab initio RHF/6-31G* calculations of Wiest and Houk were used for the pseudodiequatorial and pseudodiaxial conformers of chorismate and for the transition structure. Free energy perturbation calculations yielded the differences in free energies of solvation for the three structures. The calculations reproduce the observed 100-fold rate increase in water over methanol. The origin of the rate difference is traced solely to an enhanced population of the pseudodiaxial conformer in water, which arises largely from a unique water molecule acting as a double hydrogen bond donor to the C4 hydroxyl group and the side-chain carboxylate. A Monte Carlo simulation was also carried out for the transition structure bound to *E. coli* chorismate mutase in order to characterize the key interactions in the active site. Consistent with earlier computational results for the Claisen rearrangement of allyl vinyl ether and inferences from crystal structures, the Monte Carlo simulations reveal two hydrogen bonds to the enolic oxygen in the transition structure for both the uncatalyzed reaction in water and the enzyme-catalyzed rearrangement.

Introduction

The rearrangement of chorismate to prephenate is a key step in the biosynthesis of aromatic amino acids for various bacteria, plants, and fungi (Scheme 1).[1] Interest in the enzymatic process is multifaceted. Since the biosynthetic pathway does not exist in mammals, its inhibitors are possible leads to novel herbicides, fungicides, and antibiotics.[2] The reaction is formally a Claisen rearrangement and represents the only well-established case of an enzyme-catalyzed pericyclic reaction.[3] The enzyme, chorismate mutase (CM), actually provides relatively modest acceleration, e.g., $2-3 \times 10^6$ times the background rate.[4] There has been complementary work with catalytic antibodies that has provided rate enhancements up to 10^4-fold.[5] Important insights on the enzymatic reaction have been obtained from recent reports of the X-ray crystal structures from *E. coli* and *Bacillus subtilis* CM and the catalytic antibody 1F7 bound to a transition state analog.[6] A non-covalent mechanism is supported whereby the enzyme stabilizes the transition state through electrostatic interactions and hydrogen bonding.[1,6] On the computational side, there has been a combined semiempirical molecular orbital (AM1) and molecular dynamics study of the chorismate rearrangement catalyzed by *Bacillus subtilis* CM.[7] This study along with recent mutagenesis results[8] support the importance for catalysis of hydrogen bonds to the enolic oxygen in the transition state, as predicted from earlier Monte Carlo simulations of the parent Claisen rearrangement in water.[9]

Scheme 1

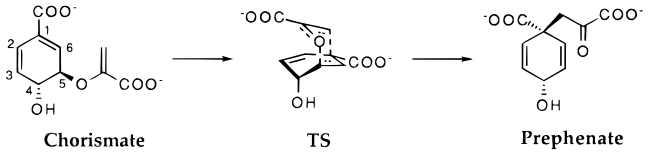

Of course, the complete picture also requires understanding mechanistic details including rates, stereochemistry, and substituent and solvent effects for the uncatalyzed rearrangement.[1] To this end, Knowles and co-workers have provided a wealth of information on both the catalyzed and uncatalyzed rearrangement of chorismate.[10] It was established that the uncatalyzed rearrangement is concerted and proceeds via a chair-like transition structure (TS). The TS is asymmetric with more advanced ether bond breakage than carbon−carbon bond formation. Also, there is an equilibrium between the pseudodiequatorial and pseudodiaxial conformers of chorismate (Scheme 2). The pseudodiequatorial form is more populated

[⊗] Abstract published in *Advance ACS Abstracts,* August 15, 1996.

(1) For a recent review, see: Ganem, B. *Angew. Chem., Int. Ed. Engl.* **1996**, *35*, 936−945.

(2) Bartlett, P. A.; Johnson, C. R. *J. Am. Chem. Soc.* **1985**, *107*, 7792−7793.

(3) Laschat, S. *Angew. Chem., Int. Ed. Engl.* **1996**, *35*, 289−291.

(4) (a) Andrews, P. R.; Smith, G. D.; Young, I. G. *Biochemistry* **1973**, *12*, 3492−3498. (b) Görisch, H. *Biochemistry* **1978**, *17*, 3700−3705. (c) Pawlak, J. L.; Padykula, R. E.; Kronis, J. D.; Aleksejczyk, R. A.; Berchtold, G. A. *J. Am. Chem. Soc.* **1989**, *111*, 3374−3381. (d) Ife, R. J.; Ball, L. F.; Lowe, P.; Haslam, E. *J. Chem. Soc., Perkin Trans. 1* **1976**, 1776−1783.

(5) (a) Jackson, D. Y.; Jacobs, J. W.; Sugasawara, R.; Reich, S. H.; Bartlett, P. A.; Schultz, P. G. *J. Am. Chem. Soc.* **1988**, *110*, 4841−4842. (b) Hilvert, D.; Carpenter, S. H.; Nared, K. D.; Auditor, M. M. *Proc. Natl. Acad. Sci. U.S.A.* **1988**, *85*, 4953−4955. Hilvert, D. *Curr. Opin. Struct. Biol.* **1994**, *4*, 612−617.

(6) (a) Chook, Y.-M.; Gray, J. V.; Ke, H.; Lipscomb, W. N. *J. Mol. Biol.* **1994**, *240*, 476−500. (b) Lee, A. Y.; Karplus, P. A.; Ganem, B.; Clardy, J. *J. Am. Chem. Soc.* **1995**, *117*, 3627−3628. (c) Haynes, M. R.; Stura, E. A.; Hilvert, D.; Wilson, I. A. *Science* **1994**, *263*, 646−652.

(7) Lyne, P. D.; Mulholland, A. J.; Richards, W. G. *J. Am. Chem. Soc.* **1995**, *117*, 11345−11350.

(8) (a) Cload, S. T.; Liu, D. R.; Pastor, R. M.; Schultz, P. G. *J. Am. Chem. Soc.* **1996**, *118*, 1787−1788. (b) Liu, D. R.; Cload, S. T.; Pastor, R. M.; Schultz, P. G. *J. Am. Chem. Soc.* **1996**, *118*, 1789−1790. (c) Kast, P.; Hartgerink, J. D.; Asif-Ullah, M.; Hilvert, D. *J. Am. Chem. Soc.* **1996**, *118*, 3069−3070.

(9) (a) Severance, D. L.; Jorgensen, W. L. *J. Am. Chem. Soc.* **1992**, *114*, 10966−10968. (b) Severance, D. L.; Jorgensen, W. L. In *Structure and Reactivity in Aqueous Solution*; Cramer, C. J., Truhlar, D. G., Eds.; ACS Symposium Series 568; American Chemical Society: Washington, DC, 1994; pp 243−259.

(10) (a) Addadi, L.; Jaffe, E. K.; Knowles, J. R. *Biochemistry* **1983**, *22*, 4494−4501. (b) Copley, S. D.; Knowles, J. R. *J. Am. Chem. Soc.* **1985**, *107*, 5306−5308. (c) Copley, S. D.; Knowles, J. R. *J. Am. Chem. Soc.* **1987**, *109*, 5008−5013. (d) Guilford, W. J.; Copley, S. D.; Knowles, J. R. *J. Am. Chem. Soc.* **1987**, *109*, 5013−5019.

S0002-7863(96)01500-4 CCC: $12.00

Scheme 2

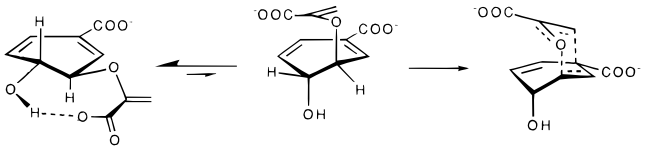

Table 1. Conformational Populations and Free Energy Differences, ΔG_0 (kcal/mol), for Chorismate, Chorismic Acid, and 4-*O*-Methylchorismate in Water and in Methanol at 25 °C[a]

	% pseudodiequatorial (ΔG_0)	
molecule	water	methanol
chorismate	~88 (1.2)	>98 (>2.3)
chorismic acid	~83 (0.9)	~87 (1.1)
4-*O*-methylchorismate	~60 (0.2)	~65 (0.4)

[a] Populations from ref 10c.

because its stability is enhanced by formation of an internal hydrogen bond between the hydroxyl group and the side-chain carboxylate. However, a pseudodiaxial structure is the reactive conformer capable of progressing to the TS. The observed binding sites that snuggly accommodate the TS mimic in the X-ray structures[6] have supported the proposal that CMs selectively bind the pseudodiaxial conformer.[10] However, the binding site of *B. subtilis* CM does reveal a flexible C-terminal tail, which rigidifies upon binding the TS mimic.[6a] Thus, it is possible that some conformational change occurs for the bound substrate such as conversion of an initial pseudodiaxial conformer to a more reactive TS-like form.

Interesting solvent effects on the pseudodiequatorial/pseudodiaxial equilibrium for chorismate, chorismic acid, and 4-*O*-methylchorismate were also found by Copley and Knowles, as summarized in Table 1.[10c] The tetrabutylammonium counterions for chorismate in the experiments are expected to yield full dissociation in the protic solvents at the low concentrations that were used, 0.8 mM.[10c] For the experiments in water with chorismic acid, the diprotonated form was maintained by addition of 0.1 N DCl.[10c] The pseudodiequatorial conformer is preferred in all cases, and the equilibrium constants are similar for the latter two substrates in both water and methanol. However, chorismate has a relatively larger pseudodiaxial population in water than methanol; in fact, none of the pseudodiaxial conformer was detected by NMR in methanol. Two possible explanations for the relatively higher pseudodiaxial population in water were provided: (1) water is a more polar solvent than methanol and may reduce the Coulombic repulsion of the two carboxylates, which were presumed to be closer in the pseudodiaxial conformer, and/or (2) water is more competitive in breaking the internal hydrogen bond than methanol. However, the data for 4-*O*-methylchorismate were interpreted to support the latter proposal. The Coulombic term is still present for this substrate, so loss of the internal hydrogen bond must then be responsible for the substantial increase in the pseudodiaxial population in both methanol and water. For chorisimic acid, the internal hydrogen bond to the carboxylic acid group is not as strong as to the carboxylate in chorismate and it has an intermediate pseudodiaxial population.

In addition, the overall rates of rearrangement were found to be faster in water than in methanol.[10c] At 50 °C, the rate in water was faster by 100-fold for chorismate, 11-fold for chorismic acid, and 7-fold for 4-*O*-methylchorismate.[10c] The factors contributing to these solvent effects cannot be unequivocally sorted out from the experimental data. Copley and Knowles proposed that 10-fold of the 100-fold rate enhancement for chorismate in water was due to the skewed equilibrium; the other 10-fold was attributed to greater stabilization in water for the TS of the rearrangement. The TS was assumed to be more polar than the reactant, taking on some character of a tight ion pair between an enol pyruvate anion and a cyclohexadienyl cation.[10c] Solvent effects on other Claisen rearrangements are also significant;[1] e.g., a factor of 23 rate enhancement was obtained for the switch from methanol to water for a 4-hexamethylenecarboxylate derivative of allyl vinyl ether.[11] Though the rate increase for chorismate was noted as particularly large, the rate increases and secondary isotopic effects are still significantly less than for reactions such as solvolyses that feature heterolytic bond cleavage.[11]

Valuable insights have also been obtained for the uncatalyzed reaction from ab initio molecular orbital calculations. Wiest and Houk characterized the reaction path for the rearrangement of chorismate and analogs in the gas phase with ab initio calculations at the RHF/6-31G* and BLYP/6-31G* levels,[12] while Davidson and Hillier examined the rearrangement of chorismic acid at the RHF/6-31G* level.[13] Inspection of the chorismate conformers determined from the RHF/6-31G* calculations may explain the rather small influence of intercarboxylate Coulombic repulsion on the pseudodiequatorial/pseudodiaxial equilibrium (Figure 1). There is little change in the distance between the carboxylate groups upon interconverting the two conformers. This is an interesting point because the pseudodiaxial conformer is frequently depicted as similar to the TS, as in Scheme 2.[1,6b,c,10] Though multiple orientations of the side chain are possible, the ab initio structure for the pseudodiaxial form is more extended than the suggested TS-like conformation. However, no energy minimum for a TS-like pseudodiaxial conformer could be located at the RHF/6-31G* level.[12a] Of course, solvation may significantly affect the conformational energetics.

In order to help clarify the origin of the solvent effects on both the pseudodiequatorial/pseudodiaxial equilibrium and the rate of the uncatalyzed reaction, the present Monte Carlo simulations were undertaken to follow the rearrangement in both methanol and water. A particular target was to establish if the structures and charge distributions from the ab initio 6-31G* calculations of Wiest and Houk[12] would yield solvent effects in line with the observations of Copley and Knowles.[10c] This could shed light on the structure of the pseudodiaxial conformer in solution and on the partitioning of the 100-fold slower rate in methanol between the shift in the equilibrium and solvation of the transition state. The work follows our earlier studies that demonstrated the importance of enhanced hydrogen bonding in the TS for the Claisen rearrangement of allyl vinyl ether.[9] Studies by others have supported this finding and the greater importance of charge polarization in the TS than partial ionization.[14] We also report Monte Carlo results depicting the transition structure in the active site of *E. coli* chorismate mutase.

Computational Details

The calculations in water and methanol were performed with the BOSS program[15] using intermolecular potential functions in the OPLS

(11) Brandes, E.; Grieco, P. A.; Gajewski, J. J. *J. Org. Chem.* **1989**, *54*, 515−516.
(12) (a) Wiest, O.; Houk, K. N. *J. Org. Chem.* **1994**, *59*, 7582−7584. (b) Wiest, O.; Houk, K. N. *J. Am. Chem. Soc.* **1995**, *117*, 11628−11639.
(13) Davidson, M. M.; Hillier, I. H. *J. Chem. Soc., Perkin Trans. 2* **1994**, 1415−1418.
(14) (a) Cramer, C. J.; Truhlar, D. G. *J. Am. Chem. Soc.* **1992**, *114*, 8794−8799. (b) Gao, J. *J. Am. Chem. Soc.* **1994**, *116*, 1563−1564. (c) Davidson, M. M.; Hillier, I. H. *J. Phys. Chem.* **1995**, *99*, 6748−6751. (d) Sehgal, A.; Shao, L.; Gao, J. *J. Am. Chem. Soc.* **1995**, *117*, 11337−11340.
(15) Jorgensen, W. L. *BOSS, Version 3.6*, Yale University: New Haven, CT, 1995.

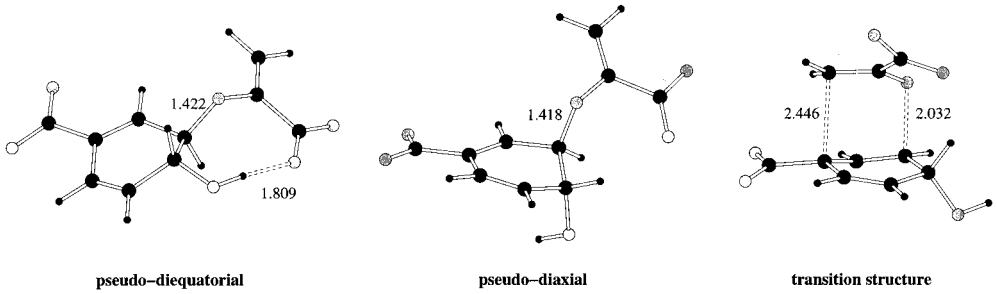

Figure 1. Wiest and Houk's chorismate structures determined with RHF/6-31G* calculations.[12]

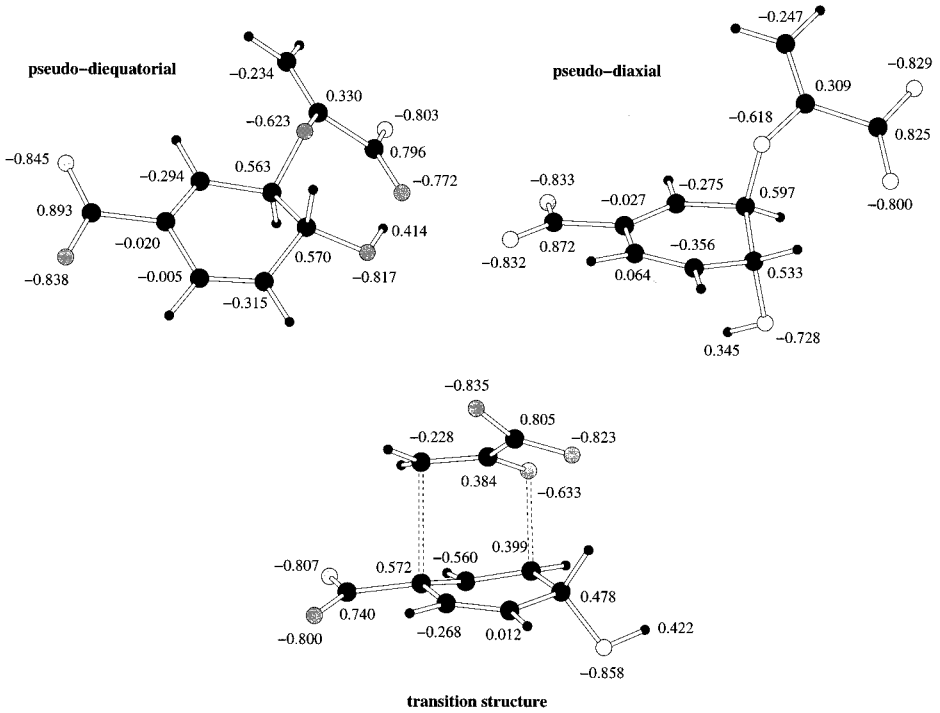

Figure 2. Partial charges for the chorismate structures. For clarity, the charges for hydrogens have been summed onto the adjacent carbons.[12] Complete force-field parameters are in the supporting information.

format.[16] The potential energy of the system is determined as a sum of two-body interactions, eq 1. The contribution of two molecules, E_{ab}, where a and b can be either solute or solvent, is defined by Coulombic and Lennard-Jones interactions between each atom *i* in a and *j* in b, eq 2. All calculations utilized the RHF/6-31G* geometries

$$E_{\text{total}} = \sum_{a<b} E_{ab} \tag{1}$$

$$E_{ab} = \sum_{i}^{a}\sum_{j}^{b}\left\{\frac{q_i q_j e^2}{r_{ij}} + 4\epsilon_{ij}\left[\left(\frac{\sigma_{ij}}{r_{ij}}\right)^{12} - \left(\frac{\sigma_{ij}}{r_{ij}}\right)^{6}\right]\right\} \tag{2}$$

(Figure 1) and partial charges fit to the electrostatic potential surface (EPS) for the chorismate conformers and TS from Wiest and Houk.[12] Comparison of computed and experimental secondary kinetic isotope effects indicates that the RHF/6-31G* geometry of the TS is more accurate than the BLYP/6-31G* alternative.[12b] It appears that the computed breaking C−O distance of 2.03 Å is close to the true value in water, while the forming bond is probably near 2.6 Å, i.e., somewhat longer than the computed 2.45 Å.[12b] A table in the supporting information lists the partial charges and Lennard-Jones parameters for the three structures. The partial charges are also illustrated in Figure 2. The Lennard-Jones parameters are OPLS all-atom values taken from earlier work.[9,16] For the solvents, the four-site TIP4P and three-site OPLS models were used for water[17] and methanol,[18] respectively.

Monte Carlo statistical mechanics simulations were performed to determine the differences in free energies of solvation for the three chorismate structures via Zwanzig's perturbation expression, eq 3.[19]

$$\Delta G_{AB} = G_B - G_A = -k_B T \ln\langle \exp[-(E_B - E_A)/k_B T]\rangle_A \tag{3}$$

In this equation, the average refers to sampling configurations for the reference state A, k_B is the Boltzmann constant, T is the temperature, and E_A and E_B are the total potential energies for states A and B.[20] Two series of free energy perturbation (FEP) calculations were performed in both water and methanol, one to convert the pseudodiaxial to the pseudodiequatorial structure and one for the pseudodiaxial to TS conversion. This required preparing a *Z*-matrix (r, ϑ, φ internal coordinate representation) that allowed smooth transformation from one structure to the other with BOSS. A coupling parameter, λ, is used to linearly scale the internal coordinates, charges, and Lennard-Jones parameters for the starting structure at $\lambda = 0$ to the final structure at $\lambda = 1$. The structures were treated as rigid with no sampling of internal degrees of freedom. Thus, the reported free energy changes arise only from the changes in solvation. This was done, as noted above, to examine the solvent effects obtained from exactly the RHF/6-31G* structures and EPS charge distributions. An alternative view is that it

(16) Jorgensen, W. L.; Tirado-Rives, J. *J. Am. Chem. Soc.* **1988**, *110*, 1657−1666. Kaminski, G.; Duffy, E. M.; Matsui, T.; Jorgensen, W. L. *J. Phys. Chem.* **1994**, *98*, 13077−13081.

(17) Jorgensen, W. L.; Madura, J. D. *Mol. Phys.* **1985**, *56*, 1381−1392.
(18) Jorgensen, W. L. *J. Phys. Chem.* **1986**, *90*, 1276−1284.
(19) Zwanzig, R. W. *J. Chem. Phys.* **1954**, *22*, 1420−1426.
(20) For a review, see: Kollman, P. A. *Chem. Rev.* **1993**, *93*, 2395−2417.

is assumed that the internal energy changes for the solutes in water and methanol are the same and cancel from the relative solvent effects, $\Delta\Delta G_{sol}$, which are of greatest interest here.

The calculations were performed at 25 °C and 1 atm in the isothermal, isobaric (NPT) ensemble. Each of the 12 calculations for the pseudodiequatorial to pseudodiaxial FEP calculation consisted of 6-7 $\times$ 10^6 configurations of equilibration and 4 $\times$ 10^6 configurations for averaging with double-wide sampling to yield 24 individual free energy changes (windows). The conversion of the pseudodiaxial structure to the TS utilized 50 windows. The small steps between windows were needed for precision because movement of the carboxylate groups causes large changes in the solute−solvent energy, which completely determines $E_B - E_A$ in eq 3 for these systems. The step size is dictated largely by our insistence that the standard deviation (1σ) for the free energy changes in a window be below 0.1 kcal/mol, as determined by the batch means procedure with batch sizes of ca. 5 $\times$ 10^5 configurations.[21] Since the step size was smaller in the pseudodiaxial to TS calculation, less equilibration was needed; 3 $\times$ 10^6 configurations of equilibration and 4 $\times$ 10^6 configurations of averaging were used. The free energy changes for each window were computed via eq 3, and the total free energy change for a conversion is the sum of the individual ΔG_{AB}'s for each window. Counterions were not included in the simulations since the bis(tetrabutylammonium) salt of chorismate used at low concentration in the experiments is expected to fully dissociate.[10c]

The simulations in water were conducted in a ca. 36 $\times$ 36 $\times$ 39 Å periodic cell containing 1647 TIP4P water molecules. The water−water interactions were truncated at an O−O distance of 8.5 Å and the solute−water cutoff was 12 Å, based on the shortest distance between the water oxygen and chorismate's oxygens. If an intermolecular distance is below the cutoff, the interactions between all atoms in the two molecules are included. The larger solute−water cutoff was used because of the −2 charge of chorismate. The simulations in methanol were conducted in a ca. 35 $\times$ 35 $\times$ 39 Å periodic cell with 686 OPLS methanol molecules. The methanol−methanol cutoff was at an O−O separation of 10 Å and the solute−methanol cutoff was at O−O separations of 12 Å. All interactions were quadratically feathered to zero over the last 0.5 Å before the cutoff. Metropolis and preferential sampling were used, and the ranges for attempted translations and rigid-body rotations of the solutes and solvent molecules were adjusted to yield ca. 40% acceptance rates for new configurations.[21]

Results and Discussion

Free Energetics for the Solvent Effects. Figure 3 displays the free energy changes over the course of the two FEP calculations in both solvents; $\lambda = 0.0$ corresponds to the solute in the initial conformation and $\lambda = 1.0$ corresponds to the final structure. The smoothness of the curves is an auspicious sign for the precision of the results and reflects the benefits of using the large number of windows and lengthy equilibration periods. Table 2 summarizes the cumulative changes in free energies of solvation for the pseudodiequatorial to pseudodiaxial conversion and rearrangement to the TS. The small statistical uncertainties in the individual free energy changes for each window cause the total uncertainties for the cumulative values in Table 2 to be modest, i.e., 0.2−0.7 kcal/mol as obtained from the batch means procedure. The pseudodiequatorial to pseudodiaxial mutation was performed a second time in both solvents with some details in the **Z**-matrix changed; the results were the same as those in Table 2 within 0.1 kcal/mol.

For both transformations, the free energy of solvation is expected to become more favorable. Release of the internal hydrogen bond in the pseudodiequatorial conformer (Figure 1) frees the side-chain carboxylate group for additional hydrogen bonding with solvent molecules. Then, the pivoting about the breaking C-O bond in progressing from the pseudodiaxial conformer to the transition structure brings the two carboxylate

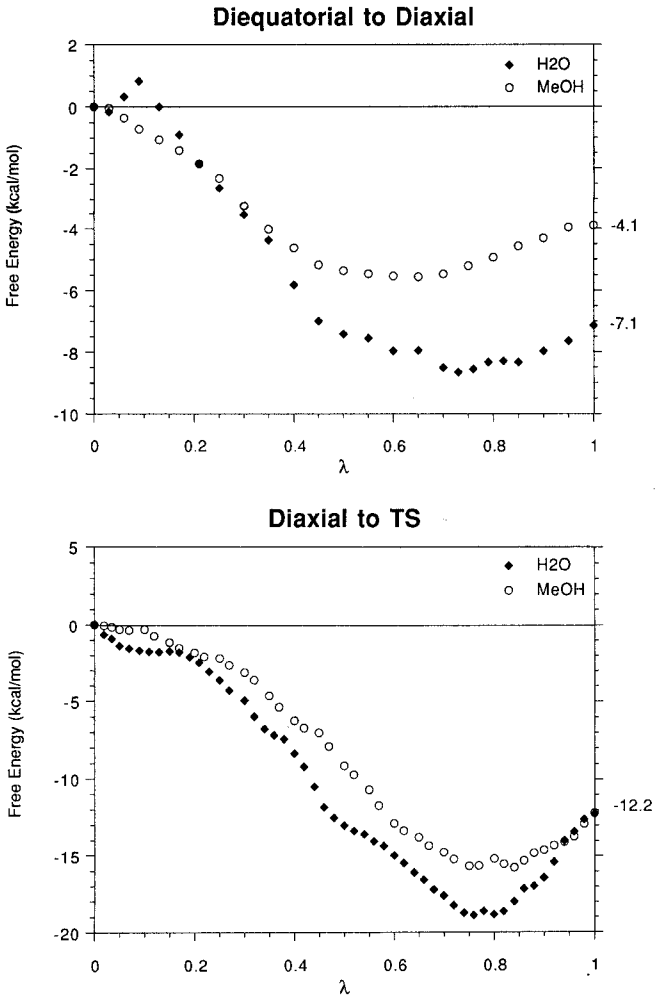

Figure 3. The free energy changes over the course of each perturbation. λ is a coupling parameter where 0.0 corresponds to the initial conformer and 1.0 corresponds to the final structure.

Table 2. Computed Changes in Free Energies of Solvation (kcal/mol) for the Chorismate to Prephenate Rearrangement

	dieq $\xrightarrow{A}$ diax $\xrightarrow{B}$ TS		
solvent	ΔG_{sol}(**A**)	ΔG_{sol}(**B**)	ΔG_{sol}(Tot.)
methanol	-4.1 ± 0.2	-12.2 ± 0.5	-16.3 ± 0.5
water	-7.1 ± 0.3	-12.2 ± 0.6	-19.3 ± 0.7
$\Delta\Delta G_{sol}$(MeOH−H_2O)	3.0 ± 0.4	0.0 ± 0.8	3.0 ± 0.9

groups closer together, which enhances long-range electrostatic interactions with the solvent. In the extreme, the quadratic dependence of the free energy of solvation of an atomic ion on its charge in the Born equation implies that a doubly-charged ion (coincident charges) has twice the solvation energy as two separate singly-charged ions.[22] There may also be enhanced polarization in the transition structure, as in the case of the parent Claisen rearrangement,[9,14] which could lead to more favorable solvation. However, this is not clearly apparent from the charges in Figure 2. The net charge on the enol pyruvate fragment only changes from −1.36 e in the pseudodiaxial conformation to −1.33 e for the TS; however, the total charge on the two carboxylate units declines from −1.59 e to −1.72 e, which portends stronger hydrogen bonds with the solvent.

The results in Figure 3 and Table 2 confirm the expectations. The free energy of solvation is computed to be more favorable

(21) Allen, M. P.; Tildesley, D. J. *Computer Simulations of Liquids*; Clarendon Press: Oxford, U. K., 1987.

(22) (a) Rashin, A. A.; Honig, B. *J. Phys. Chem.* **1985**, *89*, 5588−5593. (b) Carlson, H. A.; Jorgensen, W. L. *J. Phys. Chem.* **1995**, *99*, 10667−10673.

for the pseudodiaxial conformer than the pseudodiequatorial one by 4.1 kcal/mol in methanol and 7.1 kcal/mol in water. The net difference of 3.0 ± 0.4 kcal/mol is consistent with the observations of Copley and Knowles (Table 1).[10c] They obtained a free energy change, ΔG_0, of 1.2 kcal/mol for pseudodiequatorial → pseudodiaxial chorismate in water. Addition of the present 3.0 kcal/mol less favorable change in the free energies of solvation in methanol yields a ΔG_0 of 4.2 kcal/mol for the equilibrium in methanol and a vanishingly small pseudodiaxial population.

Then, in both solvents, the calculations predict that the RHF/6-31G* transition structure is better solvated than the pseudodiaxial conformer by 12.2 kcal/mol. Overall, the TS is computed to be better solvated than the pseudodiequatorial reactant by 16.3 ± 0.5 kcal/mol in methanol and 19.3 ± 0.7 kcal/mol in water. The mechanistic view is that the pseudodiequatorial and pseudodiaxial forms are in rapid equilibrium and the pseudodiaxial to TS conversion is the rate determining step.[10] The overall rate constant is then the product of the equilibrium constant and the rate constant for the pseudodiaxial to product step. The free energy of activation, $\Delta G^{\ddagger}$, is the sum of the free energy change for the equilibrium, ΔG_0, and the free energy change between the pseudodiaxial conformer and the TS, ΔG_{TS}. Finally, the difference in free energy of activation in the two solvents, $\Delta\Delta G^{\ddagger}$, is the sum of the solvent effects on the equilibrium and rate determining step, $\Delta\Delta G_0 + \Delta\Delta G_{TS}$. The chorismate to prephenate reaction proceeds 100-fold faster in water than in methanol at 50 °C.[10c] This corresponds to a $\Delta\Delta G^{\ddagger}$ of 2.96 kcal/mol, which coincides with the present result of 3.0 ± 0.9 kcal/mol (Table 2).

Thus, the Monte Carlo simulations with the RHF/6-31G* structures and charges reproduce the observed shift to a higher pseudodiaxial population in water and the overall rate enhancement in water over methanol. Interestingly, the calculations indicate that the increased rate in water is due entirely to the shift in the pseudodiequatorial/pseudodiaxial equilibrium, $\Delta\Delta G_0 = 3.0 \pm 0.4$ and $\Delta\Delta G_{TS} = 0.0 \pm 0.8$ kcal/mol. It is emphasized that the principal assumptions in the computations are that the RHF/6-31G* structures and charges are valid in both solvents and that the internal energies of the solutes are the same in both solvents. In any event, the accord between the observed and computed solvent effects is striking. The origin of the solvent effects is addressed below after the absolute free energy changes are considered.

Absolute Free Energetics. In principle, the computed solvent effects can be combined with the gas-phase free energies from the ab initio calculations to yield predicted values for $\Delta G^{\ddagger}$ and ΔG_0 in methanol and water. The problem is that it is easier to obtain accurate structural results from the ab initio calculations than energetics. At the RHF level, the lack of corrections for the correlation energy causes activation energies for pericyclic reactions to be overestimated, while the incomplete treatment of the correlation energy with the BLYP calculations yields underestimates.[12,23] The inclusion of diffuse functions in the basis set, as in 6-31+G*, can also be important for the description of anions; however, the computed activation energies for a series of Claisen rearrangements for chorismate analogs were found to be insensitive to this addition.[12b] In order to bring the ab initio activation energy into agreement with experiment for the rearrangement of allyl vinyl ether in the gas phase, Wiest and Houk proposed a −16.8 kcal/mol correction for the RHF/6-31G* activation energies,[12a] while the correction would be +9.5 kcal/mol for the BLYP/6-31G* results. Wiest and Houk also performed the necessary vibrational frequency calculations at the RHF/6-31G* and BLYP/6-31G* levels and obtained the results for enthalpy and entropy changes for the chorismate rearrangement in Table 3.[24] With the above corrections, the best estimates for $\Delta G^{\ddagger}$ in the gas phase are 51.7 and 43.5 kcal/mol based on the RHF/6-31G* and BLYP/6-31G* results. As summarized in Table 4, addition of the solvent effects from Table 2 then yields computed free energies of activation in water of 32.4 ± 0.7 and 24.2 ± 0.7 kcal/mol. The BLYP-based value coincides with the observed $\Delta G^{\ddagger}$ of 24.5 kcal/mol in water at 25 °C and pH 7.5.[4a] Therefore, the computed overall solvent effects of ca. −19 and −16 kcal/mol for the rearrangement in water and methanol are in a reasonable range.

Table 3. Computed Thermodynamic Results in the Gas Phase[a]

	RHF/6-31G*	BLYP/6-31G*
ΔH_0	11.7	11.5
ΔS_0	3.4	3.6
ΔG_0	10.7	10.5
$\Delta H^{\ddagger}$	50.8	44.2
$\Delta S^{\ddagger}$	−3.0	2.4
$\Delta G^{\ddagger}$	51.7	43.5

[a] Data from refs 12 and 24. Geometries were fully optimized at the indicated level. ΔH and ΔG in kcal/mol; ΔS in cal/(mol·K).

Table 4. Computed and Experimental Total Free Energy Changes (kcal/mol) in Solution[a]

	solvent	RHF/6-31G*	BLYP/6-31G*	exptl
ΔG_0	water	3.6 ± 0.3	3.4 ± 0.3	1.2
ΔG_0	methanol	6.6 ± 0.2	6.4 ± 0.2	>2.3
$\Delta G^{\ddagger}$	water	32.4 ± 0.7	24.2 ± 0.7	24.5
$\Delta G^{\ddagger}$	methanol	35.4 ± 0.5	27.2 ± 0.5	27.5

[a] Computed values at 25 °C from combining results in Tables 2 and 3. Experimental values at 25 °C for ΔG_0 and at 50 °C for $\Delta G^{\ddagger}$ from refs 4a and 10c.

For the equilibrium between the pseudodiequatorial and pseudodiaxial conformers, the gas-phase contribution to the free energy change, ΔG_0, is 10.7 kcal/mol at the RHF/6-31G* level and 10.5 kcal/mol from the BLYP calculations (Table 3). Combination with the solvent effects in Table 2 yields predicted ΔG_0 values from the RHF results that are too high by about 2 kcal/mol: 3.6 kcal/mol in water and 6.6 kcal/mol in methanol (Table 4). The predictions for ΔG_0 with the BLYP results are similar, 3.4 kcal/mol in water and 6.4 kcal/mol in methanol.

The relatively large number of heavy atoms in chorismate and its dianionic character are challenging for the ab initio calculations. The uncertainty is reflected in the discrepancies between the RHF/6-31G* and BLYP/6-31G* results in Table 3. Under the circumstances, the corrected results combined with the present relative free energies of solvation have yielded very reasonable values for the absolute ΔG_0 and $\Delta G^{\ddagger}$ in solution. However, another potential source of error in the calculations is that only one conformer has been considered for the pseudodiequatorial, pseudodiaxial, and TS forms. This issue was studied in detail for the Claisen rearrangement of allyl vinyl ether for which the reactant has nine low-energy conformers and the TS has only one.[9b] The effect of including all conformers vs just the lowest-energy one for the reactant was to raise the computed $\Delta G^{\ddagger}$ in the gas phase by 0.6 kcal/mol. For the chorismate rearrangement, it is anticipated that the

(23) For a review, see: Houk, K. N.; Li, Y.; Evanseck, J. D. *Angew. Chem., Int. Ed. Engl.* **1992**, *31*, 682−708.

(24) Wiest, O.; Houk, K. N. Personal communication. The RHF/6-31G* vibrational frequencies were scaled by 0.91 and the BLYP/6-31G* values were unscaled. Scaled frequencies below 500 cm^{-1} were treated as classical rotations in evaluating the vibrational energies. The imaginary frequency for the transition structure is ignored in computing the vibrational energy and entropy.

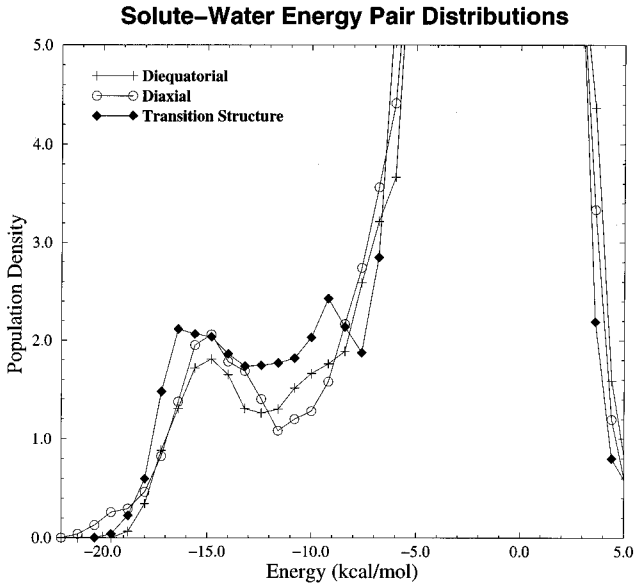

Figure 4. Distribution of individual chorismate−water interaction energies. The number of water molecules given on the *y*-axis that interact with the solute with the interaction energy shown on the *x*-axis. Units for the *y*-axis are no. of molecules per kcal/mol.

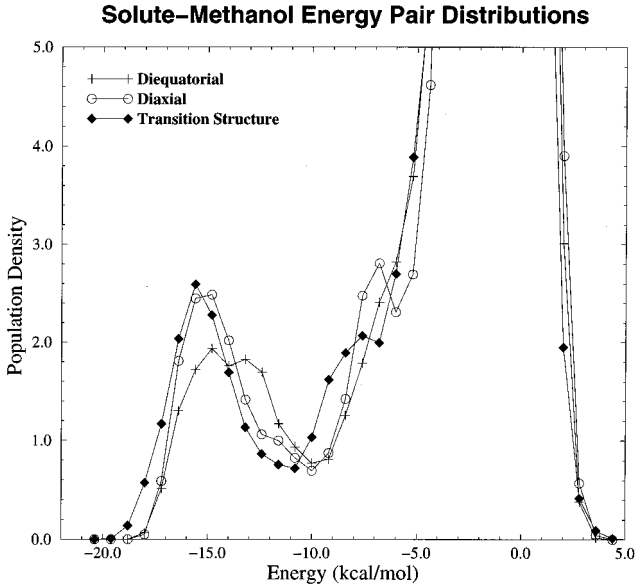

Figure 5. Distribution of individual chorismate−methanol interaction energies. The number of methanol molecules given on the *y*-axis that interact with the solute with the interaction energy shown on the *x*-axis. Units for the y-axis are no. of molecules per kcal/mol.

internally hydrogen-bonded pseudodiequatorial reactant is the only low-energy conformer so the gas-phase $\Delta G^{\ddagger}$ and its components, $\Delta H^{\ddagger}$ and $\Delta S^{\ddagger}$, should not be affected by including multiple conformers. On the other hand, the pseudodiaxial structure has more conformational freedom about the two bonds to the ether oxygen and the C4−OH bond. Crudely, models suggest that this might allow population of a total of 8 conformers without getting the two carboxylates too close; the maximum entropic effect of R ln 8 could then lower the free energy of the pseudodiaxial form by 1.2 kcal/mol, which would bring the computed ΔG_0 values close to the experimental results. With this consideration, it appears that the combined ab initio and Monte Carlo results are giving a complete picture for the chorismate rearrangement that is in good accord with the observed rate and equilibrium data in methanol and water.

Energy Pair Distributions. The key issue now is why is the pseudodiaxial structure relatively better solvated in water than methanol. To begin, solute−solvent energy pair distributions are often revealing. These are shown for the pseudodiequatorial, pseudodiaxial, and TS structures in Figures 4 and 5 for water and methanol. The plots give the number of solvent molecules on the *y*-axis that interact with the solute with the interaction energy shown on the *x*-axis. The bands at low energy result from the hydrogen-bonded solvent molecules and the spike centered at 0 kcal/mol comes from the weak interactions between the solute and the many distant solvent molecules. The distributions are computed on-the-fly in BOSS and are averaged over 4×10^6 configurations. In both solvents, there is a particularly strongly bound group of solvent molecules, which form a band from ca. −10 to −20 kcal/mol. Integration of the band reveals 10.5, 11.7, and 14.0 water molecules for the pseudodiequatorial, pseudodiaxial, and TS structures in Figure 4 and 10.3, 11.0, and 11.2 methanol molecules for these structures in Figure 5. It should be noted that prior results have established that the normal numbers of hydrogen bonds for unencumbered functional groups in water are 2−3 for an alcohol, 1 for an ether, and 6 for a carboxylate, while the usual numbers of hydrogen bonds in methanol are 2 for an alcohol, 1 for an ether, and 5 for a carboxylate.[25] Furthermore, the hydrogen-bonded energy band for acetate ion in water and methanol also covers the −10 to −20 kcal/mol range.[25b,d] Thus, the lowest-energy bands in the present energy-pair distributions can be attributed to the solvent molecules hydrogen bonded to the carboxylate groups. Some finer details can be noted from the plots. (1) In both solvents, the lowest-energy band shifts to lower energy for the TS indicating a strengthening of the hydrogen bonds to the carboxylates on average, as expected above from the noted charge shifts. (2) The number of solvent molecules hydrogen bonded to the carboxylates increases by about one in both solvents in going from the pseudodiequatorial to pseudodiaxial conformation. This is reasonable to replace the lost internal hydrogen bond between the hydroxyl and carboxylate groups in the pseudodiequatorial structure. (3) The number of water molecules hydrogen bonded to the carboxylates increases notably by 2.3 in going from the pseudodiaxial structure to the TS, while the change is only 0.2 in methanol.

Increasing the integration limit to −5 kcal/mol for the energy pair distributions encompasses all strongly-attractive interactions with first and second shell solvent molecules. The results for the pseudodiequatorial, pseudodiaxial, and TS structures in water are 22.4, 24.3, and 27.4, and in methanol the corresponding numbers are 18.2, 19.4, and 20.2. The differences are mostly accounted for by the change in numbers of the solvent molecules in the −10 to −20 kcal/mol range. This implies that the mode of stabilization of the transition structure relative to chorismate is different in water and methanol. In water, the better solvation of the TS can be attributed largely to the increase in and strengthening of the hydrogen bonds to first shell solvent molecules, while in methanol the changes for the strongest interactions with the solvent along the reaction path are more modest (Figures 4 and 5). Thus, in methanol, the stabilization of the transition state is more a longer-range phenomenon owing to contributions from many distant solvent molecules. This is completely reasonable; the lower dielectric constant for methanol (33) than water (78) makes electrostatic interactions fade more slowly as a function of distance from the ionic solute.

(25) (a) Jorgensen, W. L. *J. Phys. Chem.* **1986**, *90*, 1276−1284. (b) Jorgensen, W. L.; Gao, J. *J. Phys. Chem.* **1986**, *90*, 2174−2182. (c) Jorgensen, W. L.; Nguyen, T. B. *J. Comp. Chem.* **1993**, *14*, 195−205. (d) Jorgensen, W. L. Unpublished results.

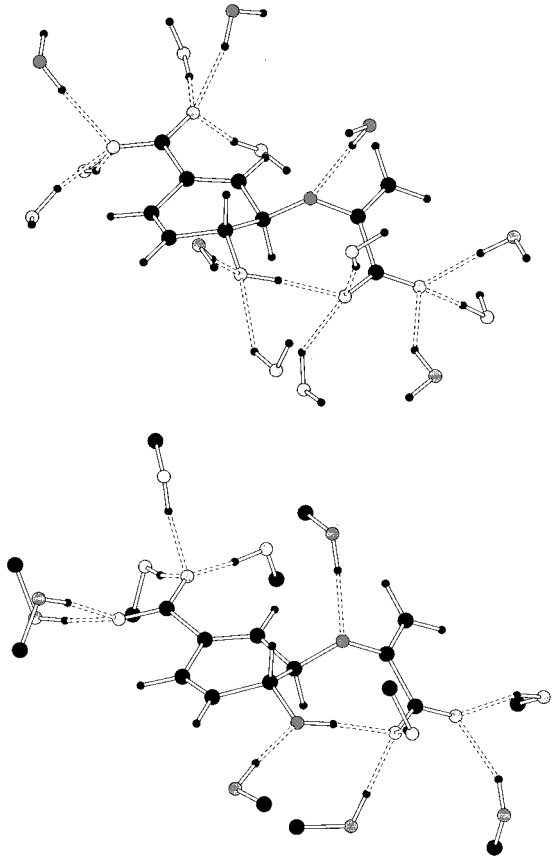

Figure 6. Illustration of one configuration from the Monte Carlo simulations for pseudodiequatorial chorismate in water (top) and methanol (bottom). All hydrogen bonds with the solute are indicated.

The issue of the relatively better solvation of the pseudodiaxial form relative to the pseudodiequatorial conformer in water than methanol can now be addressed. The energy pair distributions do indicate an increase of 1.2 strongly hydrogen-bonded neighbors in water vs 0.7 in methanol for the pseudodiaxial conformer. A more detailed look reveals an interesting feature in Figure 4. A small band occurs at −18 to −22 kcal/mol for the pseudodiaxial form in water that is not apparent in any of the other pair distribution curves in water or methanol. Integration of the feature indicates that it contains 0.6 water molecule, a water molecule that is in a uniquely favorable position for the pseudodiaxial structure. The identity of this water molecule was readily revealed from viewing configurations from the simulations and from optimizations of a single water molecule with the chorismate structures, as discussed next.

Hydrogen-Bonding Analysis. Plots of the final configurations from simulations of the three structures in both solvents are shown in Figures 6−8. For clarity, only the solvent molecules that are hydrogen bonded to the solute are shown with a hydrogen bond defined by an O···H distance less than 2.6 Å. The hydrogen-bonding patterns in the plots are typical and are consistent with the above discussion. Starting with the pseudodiequatorial structures, both carboxylates in methanol (Figure 6, bottom) participate in the expected five hydrogen bonds with one coming from the C4 hydroxyl group of chorismate. The C4 hydroxyl participates in the normal two hydrogen bonds, one as donor and one as acceptor, and the ether oxygen has one hydrogen-bonded methanol molecule. In water, the pseudodiequatorial structure (Figure 6, top) has six hydrogen bonds to both carboxylate groups, the C4 hydroxyl group is in three hydrogen bonds, and the ether oxygen again has one hydrogen-bonded solvent molecule. There is nothing unusual in these structures.

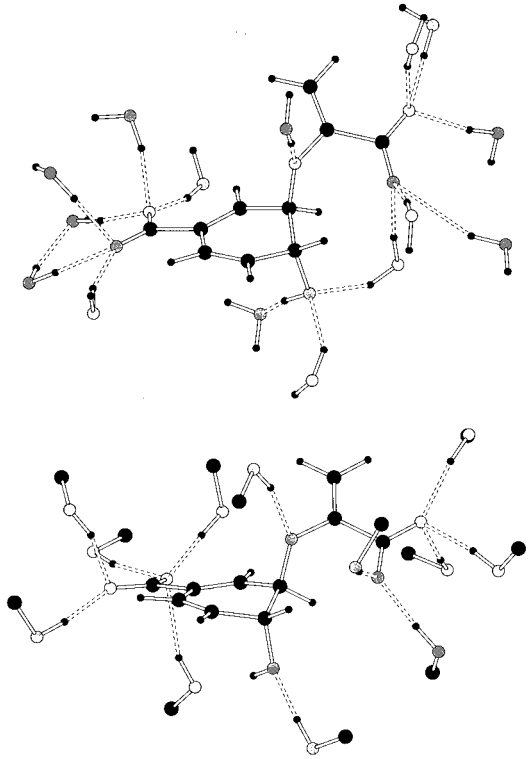

Figure 7. Illustration of one configuration from the Monte Carlo simulations for pseudodiaxial chorismate in water (top) and methanol (bottom). All hydrogen bonds with the solute are indicated.

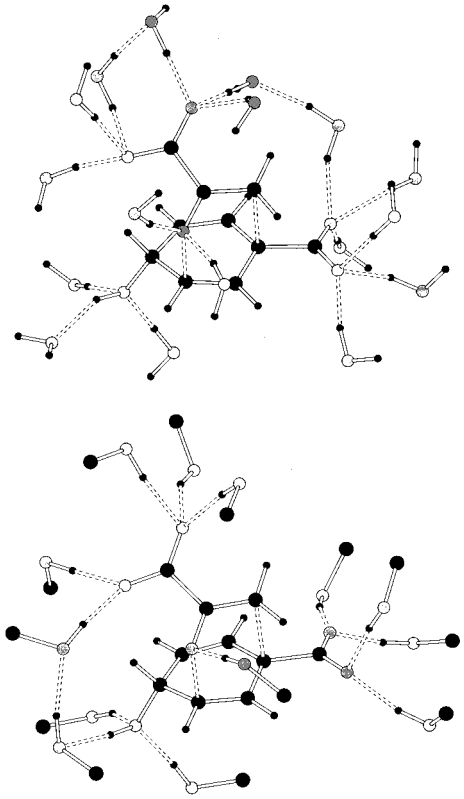

Figure 8. Illustration of one configuration from the Monte Carlo simulations for the transiiton structure in water (top) and methanol (bottom). All hydrogen bonds with the solute are indicated.

The hydrogen bonding for the pseudodiaxial structures is shown in Figure 7. In methanol, both carboxylates are still acceptors for five hydrogen bonds each with a methanol molecule replacing the lost internal hydrogen bond. The C4 hydroxyl group is accepting a hydrogen bond from one methanol

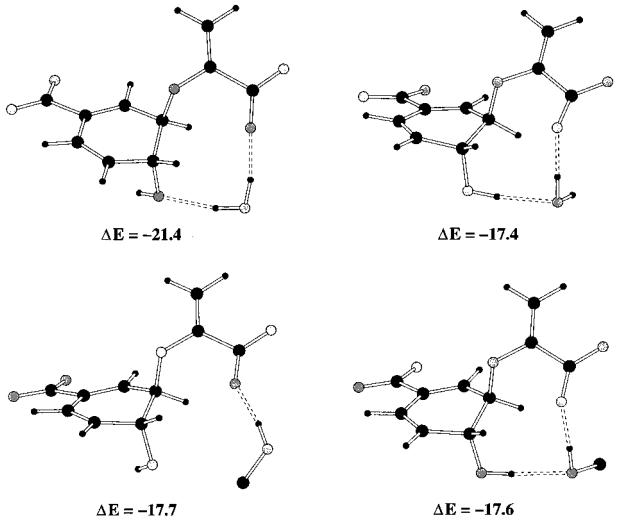

Figure 9. Results of gas-phase optimizations for a single water (top) or methanol (bottom) molecule interacting with two rotamers for pseudodiaxial chorismate. The intermolecular interaction energies are given in kcal/mol.

molecule and there is also one hydrogen bond to the ether oxygen, which gives a total of twelve hydrogen bonds. The number of hydrogen-bonded methanols increases by one in going from the pseudodiequatorial to pseudodiaxial structure owing to replacement of the internal hydrogen bond. In water, the pseudodiaxial structure has six hydrogen-bonded solvent molecules for both carboxylate groups, and the C4 hydroxyl and ether groups still participate in three and one hydrogen bonds, respectively. *The striking feature is the water molecule that is bridging between the C4 hydroxyl group and side-chain carboxylate as a double hydrogen-bond donor.* Optimizations confirmed that this is the most strongly bound water molecule that gives the interaction energies in the −18 to −22 kcal/mol range. Of course, methanol cannot function as a double hydrogen-bond donor, so an analogous bridging arrangement is not possible. The bridging water emerges as the key to the stabilization of the pseudodiaxial structure in water. It is worth noting that in the crystal structure of chorismic acid, the molecule is in the pseudodiequatorial form, and though there is not an internal hydrogen bond, there is a water molecule bridging between the C4 hydroxyl group in one monomer and a carboxyl oxygen of the side chain in another chorismic acid molecule.[26]

At this point, concern could be expressed for the orientation of the hydroxyl group in the pseudodiaxial structure from the ab initio calculations; this is the only orientation that yielded a pseudodiaxial minimum.[12] If the hydroxyl hydrogen were rotated 120°, then possibly a methanol or water molecule could bridge as a hydrogen-bond acceptor for the C4 hydroxyl hydrogen and donor to the carboxylate group. This notion was pursued through optimizations with the present potential functions of a single water or methanol molecule with the hydroxyl hydrogen rotated 120°. The key results are shown by the energy-minimized structures in Figure 9; the ΔE value is the intermolecular energy change for bringing the chorismate structure and the solvent molecule together from infinite separation. For water, the optimal double-donor arrangement is attractive by 21.4 kcal/mol, while the optimal donor/acceptor geometry is attractive by only 17.4 kcal/mol. For methanol, a single hydrogen bond to the enol pyruvyl carboxylate group is attractive by 17.7 kcal/mol and there is little change in interaction energy (17.6 kcal/mol) in going to the donor/acceptor bridging structure. The donor/acceptor structures suffer from a poor geometry for the hydrogen bond with the C4 hydroxyl group including an H···OH angle near 90°. The two hydrogen bonds for water in the double donor arrangement are more ideal; furthermore, this orients both water hydrogens toward the dianionic solute, an electrostatically very favorable situation. From viewing configurations and from the energy-pair distribution, the bridging water molecule is present more than half the time. The rest of the time two waters bridge from the C4 hydroxyl group to the carboxylate, OH···Water1···Water2···O^- with Water1 as a donor/acceptor and Water2 as a double donor. Thus, it may be concluded that the increased pseudodiaxial population in water is directly related to water's ability to act as a double hydrogen-bond donor, which allows for particularly favorable simultaneous solvation of the C4 hydroxyl and enol pyruvyl carboxylate groups in pseudodiaxial chorismate. It follows that the difference in Claisen rearrangement rates between water and other solvents should be diminished in the absence of the C4 hydroxyl group and brought more into line with observations for other allyl vinyl ethers.[1,10c,11]

The hydrogen bonding for the transition structure is illustrated in Figure 8. In the instantaneous picture in Figure 8, the carboxylate groups have four and five hydrogen-bonded methanols, the hydroxyl group has three, and the ether oxygen has one, which totals thirteen hydrogen bonds. A quantitative hydrogen-bonding analysis was performed on 80 evenly-spaced configurations from each simulation and supports the patterns that have been presented. For the TS in methanol, this analysis yielded five hydrogen bonds for each carboxylate, one for the ether oxygen, and an average of 2.7 for the C4 hydroxyl group. Thus, the reorientation of the C4 hydroxyl group does increase the number of hydrogen bonds between it and methanol molecules by 1−2. This relatively high value for a hydroxyl group in an alcohol solvent probably stems from the hydroxyl group's participation in the network with two methanol molecules that bridges to the side-chain carboxylate, as illustrated in Figure 8.

In water, the quantitative analysis and the structure in Figure 8 both reveal six water molecules hydrogen bonded to each carboxylate group, three hydrogen bonds with the C4 hydroxyl group, and two with the ether oxygen for a total of 17. Thus, compared to the pseudodiequatorial structure and consistent with the results form the energy pair distributions, there has been an increase of hydrogen-bonded water molecules by three; one for both the C4 hydroxyl and side-chain carboxylate groups replaces the internal hydrogen bond, and one new hydrogen bond emerges for the ether oxygen. The latter would be surprising, if it were not for the earlier results for the Claisen rearrangement of allyl vinyl ether, which also shows the gain of a hydrogen bond on the enolic oxygen in going from reactant to TS.[9] This results from enhanced negative charge on the oxygen and the lengthening of the breaking C−O bond, which increases the oxygen's solvent exposure.[9]

Comparison with the *E. Coli* Crystal Structure. As noted previously,[1] it was subsequently found that two hydrogen bonds occur with the analogous oxygen in the transition-state mimic bound to the active sites of *E. coli* and *Bacillus subtilis* CM.[6a,b] In order to gain insight into the accommodation of the actual chorismate TS by an enzyme, a Monte Carlo simulation was performed for the RHF/6-31G* TS bound to *E. coli* CM. The Monte Carlo simulations started from the crystal structure of *E. coli* CM[6b] with the RHF/6-31G* TS overlaid on Bartlett's inhibitor. A 20 Å cap centered on the ligand containing 615 TIP4P water molecules and the 136 protein residues nearest to

(26) Afshar, C.; Jaffe, E. K.; Carrell, H. L.; Markham, G. D.; Rajagopalan, J. S.; Rossi, M.; Glusker, J. P. *Bioorg. Chem.* **1992**, *20*, 323−333.

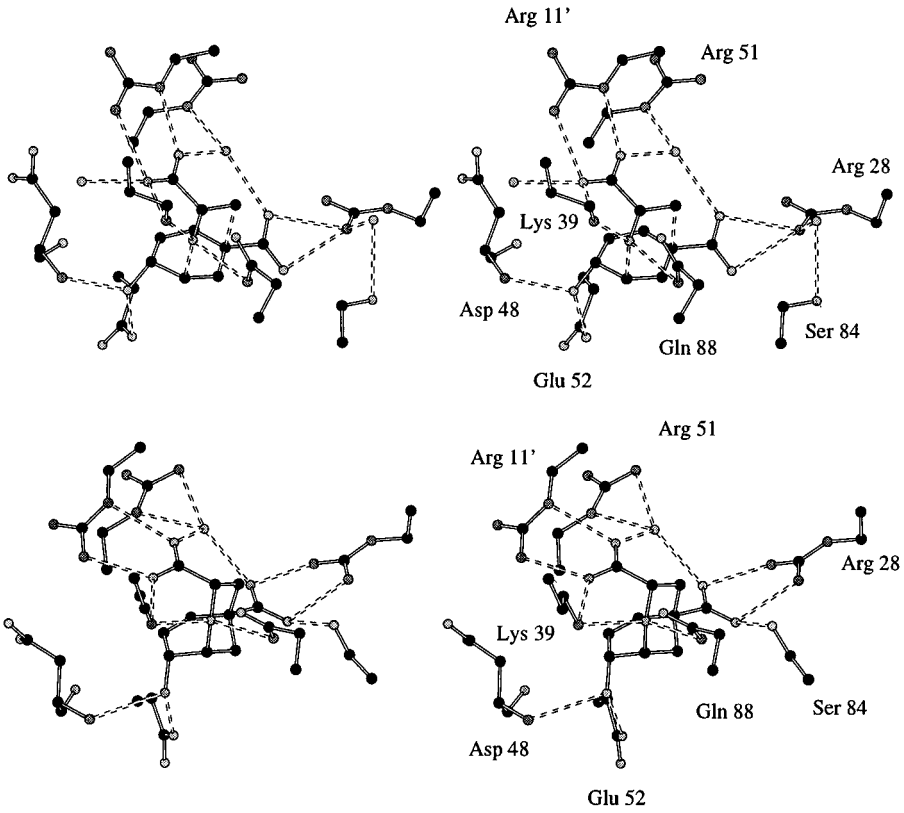

Figure 10. Stereoplots of a configuration from a Monte Carlo simulation for the chorismate transition structure in the active site of *E. coli* chorismate mutase (top) and from the crystal structure with the bound transition state mimic (bottom).[6b] All hydrogen bonds with the ligands are indicated. Hydrogen atoms are not shown for clarity.

the ligand were included in the simulation. Initial placement of the water molecules came from the positions of a preequilibrated sphere of TIP4P water with a 20 Å radius; crystallographic waters were ignored. Motions for protein side chains and for the inhibitor including internal rotations for the hydroxyl and carboxylate groups were sampled using the MCPRO program.[27] The potential functions for the inhibitor were the same as used here with the addition of the three torsions; the OPLS/AMBER force field provided the remaining parameters.[16] Monte Carlo results for the full enzymatic reaction will be described elsewhere.

A stereoplot from the last configuration after 9×10^6 configurations of equilibration is shown in Figure 10 (top) along with the analogous view from the crystal structure (bottom). Only the TS or inhibitor and nearby side chains in the active site are illustrated. There is striking similarity in the accommodation of the two ligands. The principal differences in the positions of the protein side chains are (1) Arg 28 and Arg 11′ have shifted slightly so that their salt bridges to the two carboxylate groups of the ligand are not in the perfect bidentate arrangement found in the crystal strucuture and (2) Ser 84 has reoreinted so that it no longer donates a hydrogen bond to the C1 carboxylate; instead, it shares a hydrogen-bonding water molecule with Arg 28. This water molecule actually is hydrogen bonded to both the Arg side chain and carbonyl oxygen as well as Ser 84. Reorientation of the Ser OH is electrostatically favorable for the interaction with Arg 28, though the shortest Ser O−Arg N distance is 3.55 Å in this snapshot. It may also be noted that the shifting of Arg 11′ in the simulation is accompanied by a water molecule hydrogen bonding to the enol pyruvyl carboxylate of the TS.

(27) Jorgensen, W. L., *MCPRO, Version 1.3*, Yale University: New Haven, CT, 1995.

The key similarities are the following. (1) The expected two hydrogen bonds to the enolic oxygen of the TS and the analogous ether oxygen of the inhibitor are from the side chains of Gln 88 and Lys 39. The latter also forms a salt bridge with the enol pyruvyl carboxylate or mimic. The importance of these residues for catalysis has been established; mutation of either to Ala produces a ca. 10^4 drop in activity.[8b] (2) There is a water molecule bridging between the two carboxylate groups of the ligand in both structures; the O−O distances are 2.75 and 2.77 Å in the crystal structure and 2.81 and 2.90 Å for the TS. This water molecule is also hydrogen bonded to Arg 51 in both structures. It is emphasized that the water molecules migrated to the illustrated positions in the simulation; their initial placement was arbitrary, though water molecules with their oxygens within 2.5 Å of a non-hydrogen atom of the protein are removed at the start by MCPRO. For the simulations of the TS in pure water, the single bridging water molecule was replaced by a bridge with two water molecules as in Figure 8. (3) The C4 hydroxyl group is a hydrogen-bond acceptor for the NH of Asp 48 and a donor to the side-chain carboxylate of Glu 52 in both structures. It may be noted that 4-deshydroxychorismate is still a substrate for *E. coli* CM, though the rate enhancement over the background rate is only 100-fold.[4c]

Of course, the accommodation of the TS in pure water and in the enzyme is quite different (Figures 8 and 10). In particular, most of the six hydrogen bonds to each carboxylate group in water are replaced by the salt bridges with Arg 11′, Lys 39, and Arg 28. The numerous interactions with the enol pyruvyl carboxylate and proximal enolic oxygen for the TS bound to *E. coli* CM in Figure 10 are particularly striking. It is not surprising that the chorismate analog with this carboxylate changed to a methyl ester is not a substrate or inhibitor for chorismate mutases.[4c,d]

Conclusion

Overall, the solvent effects computed here for the chorismate to prephenate rearrangement are in agreement with the observed shifts in the pseudodiequatorial/pseudodiaxial equilibrium and in the reaction rates in water and methanol. The accord supports the reasonableness of the ab initio structures and partial charges computed by Wiest and Houk at the 6-31G* level.[12] The BLYP/6-31G* energetics combined with the solvent effects computed here also yield absolute free energies of activation in accord with the experimental data, while the free energy changes for the equatorial/axial equilibrium are too high by ca. 2 kcal/mol. A key point is that the results from the Monte Carlo simulations attribute the entire 100-fold rate enhancement for the rearrangement in water over methanol to the shift to a higher pseudodiaxial population in water. A principal contributor to the effect was then traced to the occurrence of a bridging water molecule that uniquely stabilizes the pseudodiaxial structure through simultaneous donation of hydrogen bonds to the C4 hydroxyl and side-chain carboxylate groups. Another significant finding is confirmation of the catalytic desirability of having two hydrogen bonds to the enolic oxygen in the transition structures for Claisen rearrangements. This was first found computationally for the parent reaction of allyl vinyl ether in water,[9] then implied by the crystal structures for *E. coli* and *Bacillus subtilis* chorismate mutase with a bound transition-state mimic,[6a,b] and now demonstrated here for both the uncatalyzed and the *E. coli* chorismate mutase catalyzed rearrangement.

Acknowledgment. Gratitude is expressed to Profs. Olaf Wiest and K. N. Houk for the ab initio structural and thermodynamic results and discussions, to Dr. Julian Tirado-Rives for computational assistance, to Prof. Jon Clardy for the coordinates of the *E. coli* CM structure, and to the National Science Foundation and Office of Naval Research for support.

Supporting Information Available: A table listing all nonbonded parameters for the three chorismate structures (2 pages). See any current masthead page for ordering and Internet access instructions.

JA961500O